Supporting Document

Part I: Questions

1. How do hot carriers, that may relax at much faster rate (via carrier-carrier and carrier-phono interaction) may affect results obtained by FROSt?

In this technique, the photoexcited solid only affects the switch created by the pump. The reconstructed pulse is free of any influence from it: this concept has been verified through characterization of the same pulse using different solid materials.

2. How thick was SiO_2 layer for the sample ($MoTe_2$)?

Vanishing signal could be due to the layer thickness that produces destructive interference for SH?

The thickness of SiO_2 layer was around 280 nm.

At this moment, we don't have any data which would support the destructive interference by SiO_2 layer. Moreover, the reported measurements for WSe_2 and MoS_2 had the same substate. But there was no issue with SH signal.

3. Did you use/engage disp-precomp to offset the pulse chirp that is accumulated in the objective (that may contain highly dispersive glass material). Is pulse broader after the objective (if you performed that measurement)?

That's correct. The induced chirp by the highly dispersive glass materials inside the microscope lead to a broader pulse. Though, in our reported measurements (in chapter 3) the fundamental pulse was not pre chirped to avoid it. However, during the early measurements with $MoTe_2$ flake (the sample with almost no signal), the fundamental pulse was pre chirped to improve the SH intensity.

4. Is it in log-scale?

Why the slope is still not 2?

No, the data is represented in arbitrary unit.

The SH signal is proportional to the square of the intensity and $|\chi^{(2)}|^2$. Therefore, as a function of the average power, we are expecting that the square root of the signal is a linear function. This is exactly what we have observed. The difference is the slope comes from structure that generates the SH and this is proportional to $|\chi^{(2)}|$ thus explaining that the slope is changing for different material structures.

5. What is the general explanation of the asymmetric broadening towards longer wavelengths?

Short answer:

Generally, in molecular gases, when the temporal duration of the pulse gets larger, it induces a larger degree of molecular alignment (enhanced nonlinearity). Moreover, the molecular alignment is delayed with respect to the pulse temporal duration as well. Association of these two effects leads to purely red shifted spectrum.

Long answer:

The nonlinear response function $R(\tau)$ of the gas includes both the electronic and nuclear contributions. The total refractive index change induced by optical pulses with intensity profile of $I(t)$ can be written as:

$$\Delta n(t) = \int R(\tau)I(t - \tau)d\tau$$

As the rotational Raman response $h_R(\tau)$ is modeled as a damped harmonic oscillator, the rotational contribution to the nonlinear index is:

$$\Delta n_{rot} = n_2 * f_R \int h_R(\tau) I(t - \tau)d\tau$$

At the same time, the change in the refractive index due to laser induced alignment is calculated by:

$$\Delta n_{rot} = \frac{N\Delta\alpha}{n_0\epsilon_0}((\cos^2\theta)(t) - \frac{1}{3})$$

Where N is the initial molecular density, $\Delta\alpha$ the polarizability difference, and n_0 is the linear refractive index at the fundamental frequency.

In a Raman active medium (like N_2 and N_2O) the molecules are not responding instantaneously to the laser intensity, and this response can be described mathematically by the delayed response function $h_R(\tau)$. Thus, $\Delta n(t)$ can be obtained as a convolution of the $h_R(\tau)$ and $I(t)$. As $h_R(\tau)$ is delayed, the convolution presents a sharp rise at the leading edge and a slow fall at the trailing edge. Consequently, the pulse overlaps temporally mainly with the leading edge of $\Delta n(t)$ which generates new frequencies at longer wavelengths, resulting in asymmetric spectra.

6. This is not obvious at all. Is there a way to see this?

("The overlap of the pulse envelope with the tail and lead edge of $\Delta n(t)$ will determine the asymmetry degree")

Basically, for a given $R(\tau)$ the convolution $\Delta n(t) = \int R(\tau)I(t-\tau)d\tau$ results in the most steepest slope for the change of refractive index ($\frac{\Delta n(t)}{dt}$) when the pulse duration is similar (red line) to $R(\tau)$ (gray line). In other words, when the pulse duration is comparable to the characteristic time of the molecular rotation, the molecules reach maximum alignment within the fastest time scale, resulting in maximum spectral broadening.
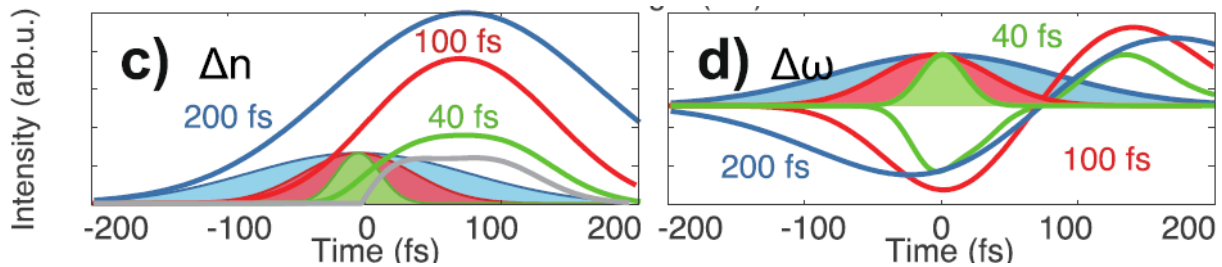

7. Which molecular rot-vibrational bands do you think are responsible for the significant broadening observed beyond 3-4GW level

The significant broadening is induced by the rotational response and Raman Gain.

8. In figure 2.8(n) phi(t) should be a linear function here and omega(t) should not be the same as in (a)

(a) Fourier limited   (b) $\phi_1 = -20$ fs   (c) $\phi_2 = 200$ fs^2
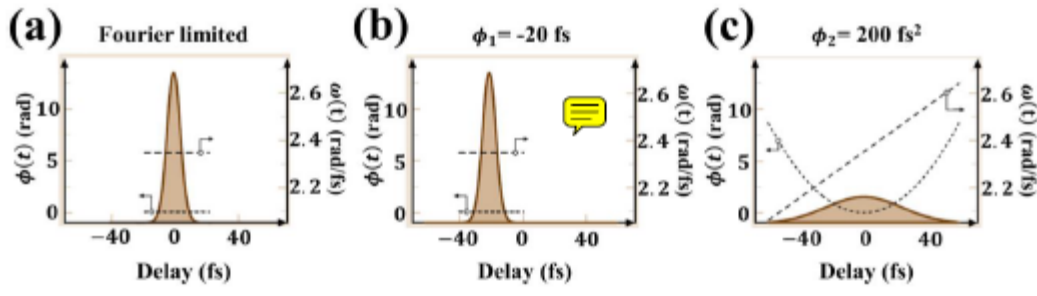
The first order phase (shifted in time for 20 fs) is only represented in terms of temporal phase and we can only observe the difference between figure 2.8(a) and (b) if we represent the spectral phase as well.
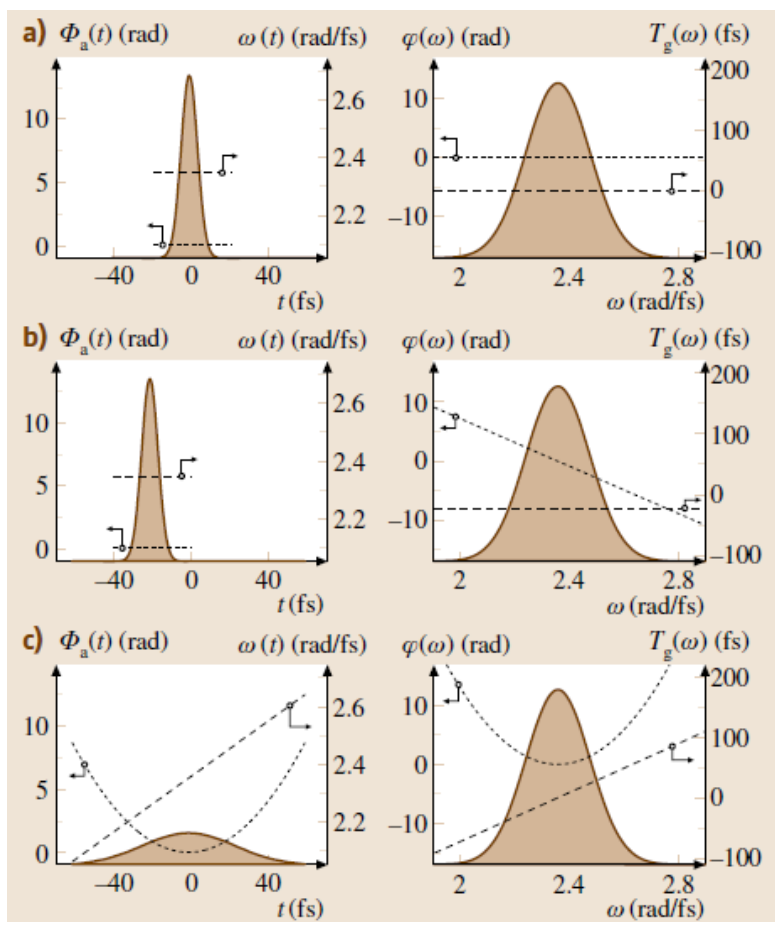
Temporal **(left)** and spectral **(right)** representation of (a): Flat phase, (b): First order phase - shifted in time, (c): Second order phase - broadened through 200 fs2 chirp.

Part II: Equations

Updated/simplified in the thesis:

Eq 6	$k_\omega = n_\omega \dfrac{\omega}{c} = n_\omega \dfrac{2\pi}{\lambda}$
Eq 8	$E(t) = \sqrt{2I(t)/\varepsilon_0 c} \; e^{i(\omega_0 t - \phi(t))}$
Eq 25	$\phi(t) = (n_0 + n_2\, I(t))k_0 L$
Eq 26	$\phi_{NL}(t) = n_2\, I(t)k_0 L = -\dfrac{2\pi}{\lambda_0}n_2 I(t)L$
Eq 27	$\omega(t) = \omega_0 + \dfrac{\partial \phi_{NL}(t)}{\partial t} = \omega_0 - \dfrac{2\pi}{\lambda_0}n_2 L \dfrac{dI(t)}{dt}$
Eq 28	$\dfrac{\partial A}{\partial z} + \dfrac{1}{2}\left(\alpha(\omega_0) + \sum_{l=1}^{\infty} i^l \dfrac{\alpha_l}{l!}\dfrac{\partial^l}{\partial t^l} \right)A - i\sum_{n=1}^{\infty} i^n \dfrac{\beta_n}{n!}\dfrac{\partial^n A}{\partial t^n}$ $= i\left(\gamma(\omega_0) + \dfrac{i}{\omega_0}\dfrac{\partial}{\partial t} \right)\left(A(z,t)\int_0^{\infty} R(t')|A(z,t-t')|^2 dt' \right)$

Part III: Figures

Updated/simplified/removed in the thesis:

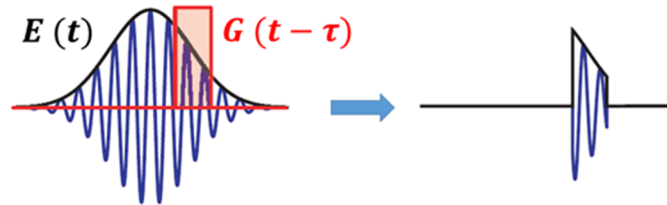Figure 2.10: Updated to avoid any confusion.

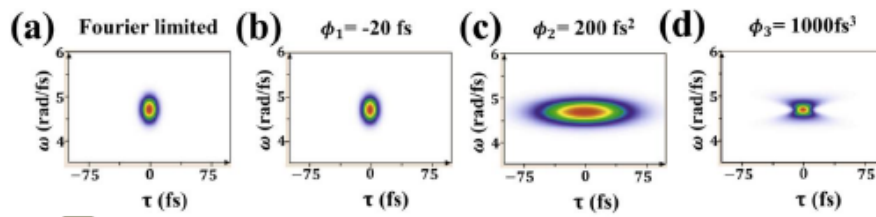Figure 2.11: Deleted to improve the readability of the thesis.

Figure 2.11: The SHG-FROG trace of 800nm Gaussian laser pulse of (a): Flat phase, (b): First order phase – shifted in time, (c): Second order phase – broadened through 200 fs² chirp (d): Third order phase. Adapted from [89].

Figure 2.21: Simplified and cited in the text.
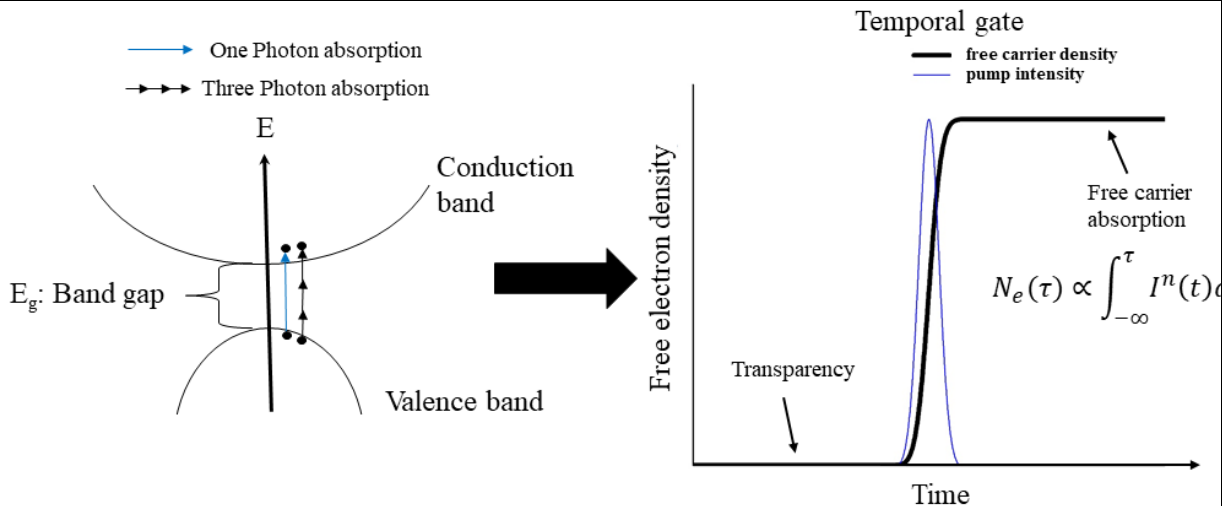
Figure 2.13: Updated.

Figure 3.13: Updated to correct the axis label.

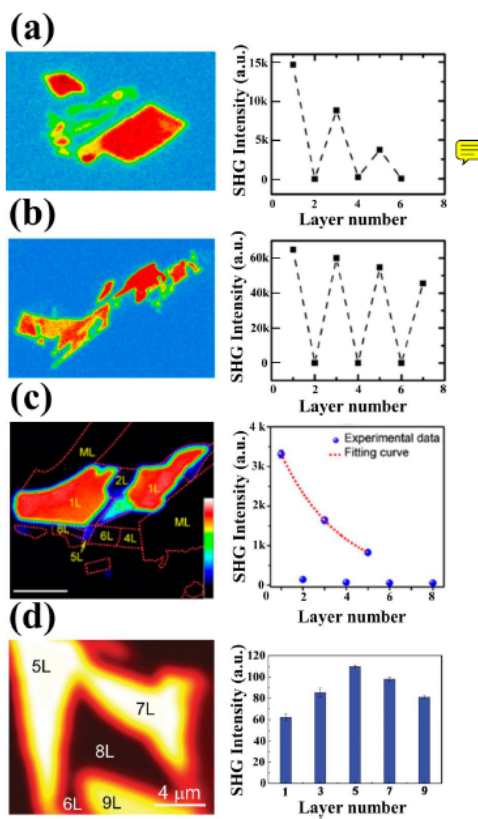**(a)**

(b)

(c)

(d)

Figure 3.13: SHG intensity of TMDs is highly depended to the layer number. The SHG image of the following TMDS is represented in right and on the left side, the SHG intensity in terms of layer number is represented. (a): WS₂ and (b): WSe₂ extracted from [205]. (c): MoS₂ extracted from [206]. (d): MoTe₂ extracted from [204].The concept of figure is adapted from [194].
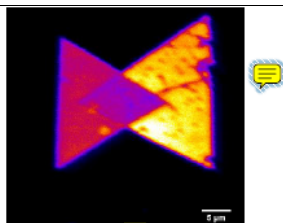
Figure 3.23: Deleted to avoid repeating the same concept.

Figure 3.23: SHG microscopy image of a p–n Heterojunctions as the reference device for our study. The left triangle is a p-type Tungsten diselenide (WSe₂) and the right triangle is a n-type Molybdenum disulphide (MoS₂). The central lozenge is the overlay of WSe₂ on MoS₂.